ARTICLE TEMPLATE

Optimal Design of Electric Machine with Efficient Handling of Constraints and Surrogate Assistance

Bhuvan Khoshoo^a, Julian Blank^b, Thang Q. Pham^a, Kalyanmoy Deb^a, and Shanelle N. Foster^a

^aDepartment of Electrical and Computer Engineering, Michigan State University, East Lansing, USA; ^bDepartment of Computer Science and Engineering, Michigan State University, East Lansing, USA

ARTICLE HISTORY

Compiled November 18, 2022

ABSTRACT

An optimal electric machine design task can be posed as a constrained multiobjective optimization problem. While the objectives require time-consuming finite element analysis, constraints, such as geometric constraints, can often be based on mathematical expressions. This article investigates this mixed computationally expensive optimization problem and proposes a computationally efficient optimization method based on evolutionary algorithms. The proposed method generates feasible solutions only by using a generalizable repair operator and also addresses the time-consuming objective functions by incorporating surrogate models for their prediction. The article successfully establishes the superiority of the proposed method over a conventional optimization approach. This study demonstrates how a complex engineering design task can be optimized efficiently for multiple objectives and constraints requiring heterogeneous evaluation times. It also shows how optimal solutions can be analyzed to select a single preferred solution and harnessed to reveal vital design features common to optimal solutions as design principles.

KEYWORDS

Electric Machine Design, Multi-objective Optimization, Surrogate-Assisted Optimization, NSGA-II, Multi-Criteria Decision Making.

1. Introduction

Electric machines are essential components within a multitude of industries today, and their range of application varies from refrigeration and industrial pumps to power generation and automobiles. Consequently, design optimization of electric machines is a complex multi-objective optimization problem (MOOP), often involving a combined electromagnetic, thermal, and structural performance analysis. Analysis of electric machines is a time-consuming process, and therefore, much effort has been focused on improving the optimization tools and efficiency in the past two decades.

From investigating pattern search and sequential unconstrained minimization techniques (Ramarathnam, Desai, and Rao 1973; Singh *et al.* 1983) to employing evolutionary algorithms (EAs) for optimization of electric machines (Bianchi and Bolognani 1998), electric machine community has continually adopted the improvements in op-

CONTACT: Bhuvan Khoshoo. Email: khoshoob@msu.edu

timization algorithms. As EAs perform better than classical direct search methods in finding global optimum, their utilization in electric machine optimization has gained further popularity (Duan, Harley, and Habetler 2009; Duan and Ionel 2013; Mirzaeian et al. 2002; Sudhoff et al. 2005; Žarko, Ban, and Lipo 2005; Zhang et al. 2013). It is also worth mentioning that electric machines require finite element analysis (FEA) for performance evaluation with high accuracy. Naturally, the application of EAs in combination with FEA can also be found in the literature (Pellegrino and Cupertino 2010a,b). Although using EAs with FEA ensures finding optimal solutions with high quality, it also increases the overall computational cost of optimization. In this regard, exploration of computationally inexpensive methods, such as surrogate models, to predict the performance of electric machines has led to a reduction in overall computational effort (Ionel and Popescu 2009; Jolly, Jabbar, and Qinghua 2005; Sizov, Ionel, and Demerdash 2012; Song et al. 2018; Taran, Ionel, and Dorrell 2018).

A comprehensive literature review shows that while efforts have been made to improve the optimization tools and efficiency, constraints handling, specifically inexpensive constraints (such as geometric), in electrical machine optimization deserves more attention. More commonly, the geometric feasibility of a candidate solution during optimization relies on random sampling. For instance, in each optimization cycle (generation), geometrically infeasible solutions are discarded, and a random initialization may be repeated until the desired number of feasible solutions has been found (Stipetic, Miebach, and Zarko 2015). However, this random sampling may be inefficient when the number of geometric variables and constraints increases. Khoshoo et al. (2021) presented a preliminary study showing that the information from inexpensive constraints can be used to repair geometrically infeasible solutions and improve the Pareto-optimal front. However, this preliminary study did not address the computational expense of the objective functions vital for electric machine design optimization. Thus, this article extends the algorithm repairing infeasible designs by incorporating surrogate models to address the time-consuming objective functions. The main contributions of this work are as follows.

- Proposal of a general repair operator that improves the quality of the Paretooptimal front by ensuring geometrically feasible solutions in each optimization
 cycle by exploiting the inexpensiveness of geometric constraints while respecting
 the manufacturing accuracy limitations.
- Performance validation of the proposed repair operator in combination with surrogates to predict the computationally expensive objective functions and their impact on the convergence of the optimization algorithm.
- Insights gained from Pareto-optimal electric machine designs and recommendations for selecting preferred solutions based on two different approaches: (1) a domain-specific a posteriori multi-criteria decision-making (MCDM) approach involving machine expertise, and (2) a systematic trade-off analysis of the obtained Pareto-optimal set.

The rest of this article is structured as follows. Section 2 discusses related work and reviews optimization methods proposed to optimize electric machine design. Section 3 discusses the formulation of the optimization problem used in this article. Section 4 presents the proposed optimization method, which exploits the computationally inexpensive constraints using a general repair operator and addresses the computationally expensive objectives by incorporating surrogate models. Following this, the impact of the algorithm's components on the algorithm's convergence, the generalizability of the

proposed repair operator, a detailed discussion about Pareto-optimal solutions, and the selection of preferred electric machine designs are presented in Section 5. Finally, conclusions are presented in Section 6.

2. Related Work

Different user applications may require electric machines with different and unique designs (Aggarwal, Strangas, and Karlis 2020; Khoshoo et al. 2022). Moreover, prolonged usage of electric machines may develop faults due to variation in machine parameters, such as vibrations (Aggarwal, Strangas, and Agapiou 2019a), current (Huang et al. 2021, 2019), and flux linkage (Aggarwal et al. 2021; Aggarwal, Strangas, and Agapiou 2019b). These faults pose a threat to user safety, and therefore, it is essential to consider multiple objectives and constraints to find optimal solutions of desired quality. In this regard, the advancements in optimization algorithms and objective function evaluation tools have facilitated the design optimization of electric machines.

Ramarathnam, Desai, and Rao (1973) presented an early case study involving an induction machine's design by solving a single objective optimization problem. The authors compared the performance of a direct, indirect, and random search method in conjunction with the sequential unconstrained minimization technique. Results showed that a direct search method performs better for complicated multi-variable functions commonly occurring in electric machines. However, optimization methods considered in the study suffered from getting stuck in local optima and required several restarts to reach the global optimum.

Metaheuristics, particularly Genetic Algorithms (GAs), are widely used and known for their global search behavior. Bianchi and Bolognani (1998) used a GA to optimize the design of a surface-mounted permanent magnet (SPM) machine. Results from two independent single objective optimization problems indicated that an evolutionary method outperforms the direct search method when comparing the convergence to the global optimum.

Since the design of an electric machine typically includes comparing the performance of multiple metrics, multi-objective optimization using EAs is predominantly employed nowadays. For instance, Pellegrino and Cupertino (2010b) employed an EA combined with FEA to solve a three-objective optimization problem. The authors compared two partial optimization strategies with a comprehensive three-objective optimization method. Results showed that domain knowledge could be utilized to modify the optimization problem creatively to reduce the computation time without significantly affecting the quality of results.

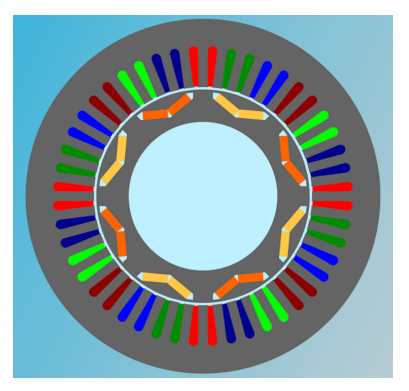
Several other strategies have been proposed for the reduction of optimization runtime. For example, Pellegrino, Cupertino, and Gerada (2015) proposed a local refinement strategy to improve a Pareto-optimal design further after the optimization terminated. After selecting a design in the region of interest, a local optimization method was employed in the design's vicinity. Results showed that an a posteriori local search, even with fewer function evaluations, produced similar results to those by an approach solely relying on global optimization. Similarly, Degano et al. (2016) split the optimization procedure into two phases, where authors optimized torque density and losses in the first stage and the quality of torque profile in the second stage. Although average torque and ripple are conflicting objectives, the optimal solutions after the second stage showed improved torque ripple without compromising the average torque.

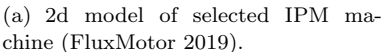
Another research direction to address computationally expensive functions during optimization is the usage of surrogate models. For example, Taran, Ionel, and Dorrell (2018) presented a two-level surrogate-assisted optimization approach using differential evolution (DE) to find optimal designs for Axial Flux PM (AFPM) machines by minimizing active material mass and total losses at rated operation. Results showed that the surrogate-assisted algorithm outperforms the conventional multi-objective DE in terms of computation time. More recently, Hayslett and Strangas (2021) presented a new analytical winding function model; it was successfully integrated with a genetic algorithm to optimize an IPM machine (Hayslett, Pham, and Strangas 2022).

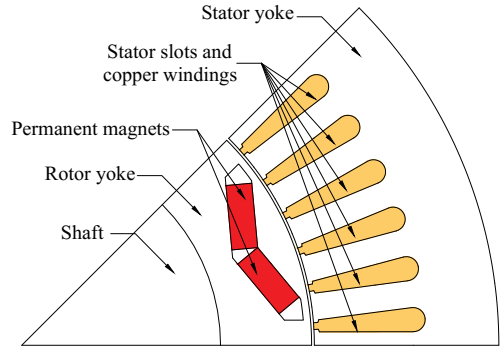
The review of related work shows that while surrogate modeling has been explored extensively, constraint handling in an electric machine design optimization problem requires more attention, especially when the constraints are inexpensive. This article addresses this gap in research by proposing a computationally efficient method to handle an electric machine design optimization problem of mixed computationally expensive nature.

3. Electric Machine Design And Optimization Problem Formulation

In addition to a selection of objective functions $(f_m, m=1,\ldots,M)$, design variables $(x_i, i=1,\ldots,N)$, variable ranges $(x_i \in [x_i^{(L)}, x_i^{(U)}]$ for all i), and constraints $(g_j, j=1,\ldots,J)$ like in every other MOOP, an electric machine design optimization problem also requires the selection of a machine template that is primarily application dependant. In this article, a 3-phase, 48-slot/8-pole IPM machine with a single layer of V-shaped magnet, used in the 2010 Toyota Prius, is chosen for analysis. In this study, two of the most common machine performance measures, Average torque and Torque pulsations, are chosen as the objective functions, which are calculated after solving a 2D transient magnetic simulation using FEA in Altair Flux software (Flux 2019). 2D model of the machine is shown in Figure 1(a) (FluxMotor 2019). Only $1/8^{th}$ of the model is simulated by taking advantage of the symmetry in the model to reduce the simulation run time, as shown in Figure 1(b). Both objective functions are conflicting, and optimization's goal is to maximize Average torque while minimizing Torque pulsations, where the definition of Torque pulsations is highlighted in Figure 2.





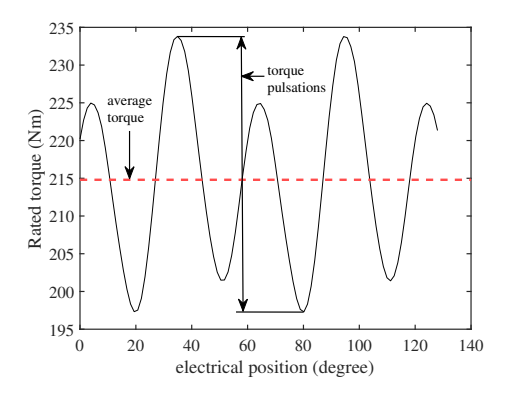


(b) Reduced model used in FEA.

Figure 1. IPM machine used for optimization

Table 1. Values of geometric variables used for optimization.

x_i	Variable Description	Unit	$x_i^{(\text{ref})}$	$x_i^{(L)}$	$x_i^{(U)}$
x_1	Height of rotor pole cap	mm	9.56	7.65	11.47
x_2	Magnet thickness	mm	7.16	5.73	8.59
x_3	Magnet width	mm	17.88	14.30	21.46
x_4	Angle between magnets	degree	145.35	116.28	174.42
x_5	Bridge height	mm	1.99	1.59	2.39
x_6	Q-axis width	mm	13.9	11.12	16.68
x_7	Slot height	mm	30.9	24.72	37.08
x_8	Slot width	mm	6.69	5.35	8.03
x_9	Height of slot opening	mm	1.22	0.98	1.46
x_{10}	Width of slot opening	mm	1.88	1.50	2.26



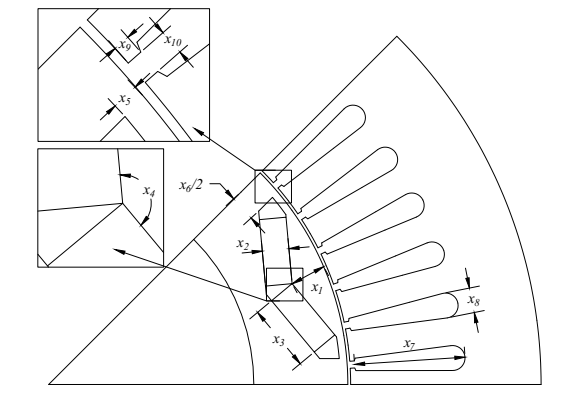


Figure 2. Torque profile of reference mahine at rated operation.

Figure 3. Geometric variables used for optimization.

After the selection of objective functions, a sensitivity analysis study has provided the ten most significant geometric variables, as shown in Figure 3. Variable ranges are defined based on the machine designer's experience with a $\pm 20\%$ variation from the reference design. Additionally, manufacturing accuracy limitations are applied to all variables by limiting them to have only two decimal places. Details of lower $(\mathbf{x}^{(L)})$ and upper $(\mathbf{x}^{(U)})$ bound vectors along with reference $(\mathbf{x}^{(\text{ref})})$ values of the ten (N=10) variables are given in Table 1. Ten geometric constraints ensure the geometric feasibility of candidate designs. All cases are analyzed at rated load and speed of the reference design. Details on the formulation of geometric constraints and the selection of the operating point for optimization are provided in the supplementary document.

Based on the above discussion of electric machine design, a bi-objective optimization problem with ten variables and ten geometric constraints is formulated in this work. Ultimately, the MOOP is defined as

$$\begin{array}{ll} \text{Maximize} & f_1(\mathbf{x}) = \texttt{Average torque}(\mathbf{x}), \\ \text{Minimize} & f_2(\mathbf{x}) = \texttt{Torque pulsations}(\mathbf{x}), \\ \text{subject to} & g_j(\mathbf{x}) \leq 0, & \forall j \in 1, \dots, J (=10), \\ & x_i^{(L)} \leq x_i \leq x_i^{(U)}, & \forall i \in 1, \dots, N (=10), \\ \text{where} & \mathbf{x} \in \mathbb{R}^N. \end{array}$$

where \mathbf{x} represent the design variables to optimize, $g_j(\mathbf{x})$ are the geometric constraints, and the lower and upper bounds of the variables are denoted by $x_i^{(L)}$ and $x_i^{(U)}$, respectively. Due to manufacturing accuracy limitations, all variables are restricted to have

only two decimal places. Additionally, while the geometric constraints are inexpensive to evaluate, objective functions require time consuming FEA.

4. Proposed Multi-Objective Optimization Algorithm

Based on the discussion presented in the previous section, it can be concluded that the formulated electric machine optimization problem is of mixed computationally expensive nature with two expensive objective functions and ten inexpensive geometric constraints. In a preliminary study, Khoshoo et al. (2021) showed that the computational inexpensiveness of constraint evaluations could be exploited to convert an infeasible solution to a feasible one through a repair operator. However, the design optimization of electric machines is an expensive problem to solve, and some effort must be made to reduce the computational cost. Therefore, in addition to the repair operator, the proposed method incorporates surrogates for predicting expensive objectives. Implementation of repair operator and surrogates in optimization algorithm is explained below.

4.1. Implementation of Repair Operator

Implementation of repair operator focuses on two goals: (1) converting an infeasible solution to a feasible one and (2) satisfying the manufacturing accuracy limitations. The two goals are achieved in two different phases, which makes the repair operator more customizable. In this work, the repair operator is combined with the evolutionary multi-objective optimization (EMO) algorithm NSGA-II (Deb et al. 2002). Although this article uses NSGA-II as the base optimization algorithm, other EMO methods can also be tried as long as the constraints used in optimization problem formulation are inexpensive to calculate.

NSGA-II is a modular, parameter-less optimization algorithm used extensively to solve bi-objective optimization problems, including electric machine design. The algorithm begins with a random sampling of solutions called the parent population. Once the parent population is evaluated, non-dominated solutions are selected (Deb 2001). The selected solutions undergo the recombination and mutation processes to create an offspring population of the same size as the parent population. Once these offspring solutions are evaluated, they are combined with the parent solutions, and the non-dominated solutions from the top half are selected as the parent population of the next generation. The process is continued till a termination criterion is reached.

4.1.1. Geometric Constraint Repair

As the name suggests, this phase converts an infeasible solution \mathbf{x} to a feasible solution \mathbf{x}' by solving an embedded optimization problem defined in (2). The feasibility of the ensuing solution \mathbf{x}' is ensured with the help of geometric and box constraints. Additionally, the objective $\|\mathbf{x} - \mathbf{x}'\|^2$ is designed to find \mathbf{x}' with the smallest Euclidean distance (in ℓ_2 -norm) to the original infeasible solution \mathbf{x} .

Minimize
$$\|\mathbf{x} - \mathbf{x}'\|^2$$
,
subject to $g_j(\mathbf{x}') \leq 0$, $\forall j \in 1, \dots, J (= 10)$,
 $x_i^{(L)} \leq x_i' \leq x_i^{(U)}$, $\forall i \in 1, \dots, N (= 10)$,
where $\mathbf{x}' \in \mathbb{R}^N$. (2)

This article uses the gradient-free simplex optimization algorithm proposed by Nelder and Mead (Nelder and Mead 1965) to solve the above optimization problem. The required initial solution is set to \mathbf{x} which makes the search focused and quick.

4.1.2. Precision Repair

The output of the first phase gives a feasible solution \mathbf{x}' . As the name suggests, the second phase modifies each variable x_i' to a floating-point number with a precision of two. To achieve this, each variable x_i' $(1 \le i \le N)$ is rounded to its floor or ceil value. This article proposes an efficient rounding scheme to choose from the 2^N neighboring possibilities.

The method first generates the sequence for rounding the variables through a random permutation P of the first N consecutive natural numbers (|P|=N). Following this, a feasible solution with two-decimal precision in all variables is found using a local search method inspired by Hooke-Jeeves pattern moves (Hooke and Jeeves 1961). For each variable under consideration, the solution's feasibility is checked by rounding that variable to its floor and ceil value. Keeping the rounding that leads to feasibility, the process is repeated for the next variable in P. If the process does not result in a feasible solution after all variables are explored, a new random permutation is attempted. A solution \mathbf{x} is discarded if it cannot be repaired in a maximum of ρ (= 100 used here) attempts.

The two phases of the repair operator are illustrated in Figure 4, which shows the feasible $(\forall j: g_j(\mathbf{x}) \leq 0)$ and the infeasible $(\exists j: g_j(\mathbf{x}) > 0)$ part of the two dimensional search space. As explained earlier, the proposed operator attempts to repair an infeasible solution \mathbf{x} in two phases. The first phase finds a feasible solution \mathbf{x}' while minimizing its Euclidean distance to \mathbf{x} . In the second phase, a new feasible solution \mathbf{x}'' is found by rounding \mathbf{x}' to a float of precision two. In the two dimensional search space (N=2), the rounding can result in $2^N=2^2=4$ different solutions, where 50% turn out to be feasible. In all possible cases, the above two phases can produce feasible solutions with two-decimal places of rounding, given that the constraints are inexpensive to evaluate.

4.2. Surrogate Incorporation in Optimization Cycle

Commonly, surrogates – approximation or interpolation models – are utilized during optimization to improve the convergence behavior. First, one shall distinguish between two different types of evaluations: exact solution evaluations (ESEs) that require running the computationally expensive evaluation for computing two objectives Average torque(x) and Torque pulsations(x); and approximate solution evaluations (ASEs), which is a computationally inexpensive approximation by the surrogates. Where the overall optimization run is limited by ESE^{max} function evaluation, function calls of

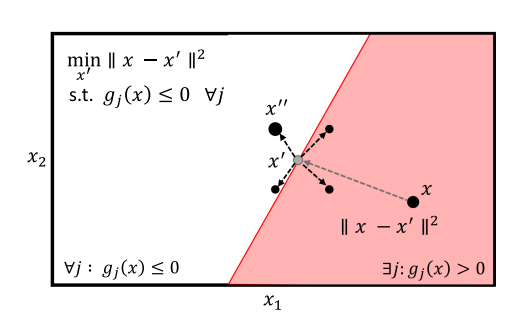


Figure 4. Illustration of the repair operator in a 2-D search space.

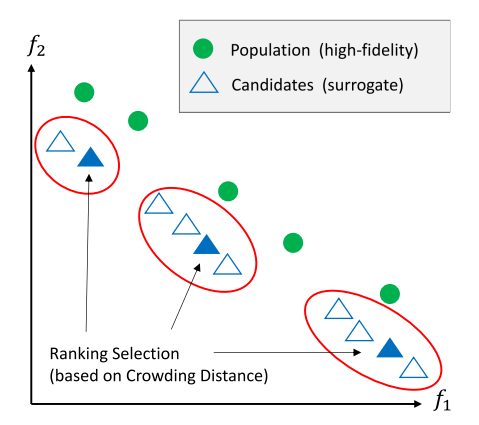


Figure 5. Ranking selection of solutions obtained by optimizing the surrogate-based optimization problem.

ASEs are only considered as algorithmic overhead. In order to improve the convergence of the algorithm, the surrogates provide ASEs and let the algorithm look several iterations into the future without any evaluation of ESEs. The surrogate models are used to create a set of infill solutions (Sasena 2002) as follows: First, NSGA-II is run for K more iterations (starting from the best solutions found so far), returning the solution set $\mathbf{X}^{(\mathrm{cand})}$. The number of solutions in $\mathbf{X}^{(\mathrm{cand})}$ corresponds to the population size of the algorithm fixed to 100 solutions in this study. After eliminating duplicates in $\mathbf{X}^{(\mathrm{cand})}$, the number of solutions N^{ESE} desired to run using ESEs needs to be selected. The selection first obtains N^{ESE} clusters by running the k-means algorithm and then uses a roulette wheel selection based on the predicted crowding distances. Note that this will introduce some selection bias towards the boundary points as they have been depicted with an infinite crowding distance. Altogether, this results in N^{ESE} solutions to be evaluated using ESEs in the current optimization cycle.

Since the electric machine design is formulated with two objectives, two different models are built. Separately fitting a model for each objective corresponds to the M1 method proposed in the surrogate usage taxonomy (Deb et al. 2019). For each objective, the best model type is found by iterating over different model realizations of RBF (Hardy 1971) and Kriging (Krige 1951) varying normalization, regression, and kernel type. Finally, the best model type is chosen based on the validation set's performance.

4.3. NSGA-II-WR-SA

Algorithm 1 shows how the repair operator and surrogate models are incorporated into the optimization cycle. The algorithm's parameters are the expensive objective functions $\mathbf{F}(\mathbf{X})$ and the inexpensive constraint functions $\mathbf{G}(\mathbf{X})$; the maximum number of exact solution evaluations $\mathrm{ESE}^{\mathrm{max}}$ serves as an overall termination criterion; the number of the initial design of experiments N^{DOE} describes how many designs are evaluated before optimization starts; the number of solutions N^{ESE} evaluated in each optimization cycle; and the number of surrogate optimization generations K, or in other words, how many generations the surrogates are used to look into the future.

First, the algorithm starts by sampling $N^{\overline{\text{DOE}}}$ solutions in the feasible space using the constrained sampling strategy (Line 1) (Blank and Deb 2021) and evaluates the

Algorithm 1: NSGA-II-WR-SA: A customized version of NSGA-II with a repair of infeasible solutions (WR) and surrogate assistance (SA).

```
Input: Expensive Objective Functions F(X), Inexpensive Constraint Function G(X),
                     Maximum Number of Exact Solution Evaluations ESE<sup>max</sup>, Number of Initial
                    Design of Experiments N^{DOE}, Number of ESEs in Each Optimization Cycle
                    N^{\text{ESE}}, Number of Surrogate Optimization Generations K.
    /* initialize feas. solutions using the inexpensive function G */ \mathbf{X} \leftarrow \texttt{constrained\_sampling}(N^{\texttt{DOE}}, \mathbf{G})
 _{2}\ \mathbf{F}\leftarrow\mathbf{F}(\mathbf{X})
 з while |X| < \mathit{ESE}^{\,\mathrm{max}} do
             /* exploitation using the surrogate */
             \hat{\mathbf{F}} \leftarrow \mathtt{fit\_surrogate}(\mathbf{X}, \mathbf{F})
              \left(\mathbf{X}^{(\mathtt{cand})}, \mathbf{F}^{(\mathtt{cand})}\right) \leftarrow \mathtt{optimize}(\texttt{'NSGA-II-WR'}, \hat{\mathbf{F}}, \mathbf{G}, \mathbf{X}, \mathbf{F}, K)
               (\mathbf{X}^{(\mathtt{cand})}, \mathbf{F}^{(\mathtt{cand})}) \leftarrow \mathtt{eliminate\_duplicates}(\mathbf{X}, \mathbf{X}^{(\mathtt{cand})}, \mathbf{F}^{(\mathtt{cand})})
  6
             C \leftarrow \texttt{cluster}(\texttt{'k\_means'}, N^{(\texttt{exploit})}, \mathbf{F}^{(\texttt{cand})})
  7
             \mathbf{X}^{(\text{infill})} \leftarrow \text{ranking\_selection}(\mathbf{X}^{(\text{cand})}, C, \text{crowding}(\mathbf{F}^{(\text{cand})}))
             /* evaluate and merge to the archive */
             \mathbf{F}^{(\text{infill})} \leftarrow \mathbf{F}(\mathbf{X}^{(\text{infill})}):
             \mathbf{X} \leftarrow \mathbf{X} \cup \mathbf{X}^{\texttt{(infill)}}
             \mathbf{F} \leftarrow \mathbf{F} \cup \mathbf{F}^{(\text{infill})}
12 end
```

solution set (Line 2). Then, while the overall evaluation budget ESE^{max} has not been used yet, surrogates $\hat{\mathbf{F}}$ are built for the objectives (Line 4). By applying NSGA-II for K surrogate optimization generations starting from \mathbf{X} , using the surrogate models $\hat{\mathbf{F}}(\mathbf{X})$ and the inexpensive objective functions $\mathbf{G}(\mathbf{X})$, a candidate set of solutions $\mathbf{X}^{(cand)}$ and $\mathbf{F}^{(cand)}$ is retrieved (Line 5). Depending on the surrogate problem, some solutions in $\mathbf{X}^{(cand)}$ can be identical to the ones already evaluated in \mathbf{X} ; thus, duplicate elimination is necessary to ensure these solutions are filtered out (Line 6). Since the size of $\mathbf{X}^{(cand)}$ exceeds N^{ESE} , a subset solution based on the predicted crowding distances takes place (Line 7 and 8). Finally, the resulting solution set $\mathbf{X}^{(infill)}$ of size N^{ESE} is evaluated using ESEs and is appended to the archive of solutions. Interested users can find more details about the implementation of surrogates by accessing *pysamoo* framework (Blank and Deb 2022).

5. Results and Discussion

In this section, the performance of the proposed optimization method is investigated and following key questions are answered.

- How does the repair operator help the optimization cycle and what is its impact on the Pareto-optimal front?
- Can the proposed repair operator be used with any EMO algorithm?
- Does the usage of surrogates improve the convergence behavior of the proposed optimization method?
- What can be learned from the Pareto-optimal solutions, each representing an electric machine design?

Table 2. Optimization Setup and Results for all five runs combined for NSGA-II and NSGA-II-WR. HV is calculated after normalization of objective functions. Set coverage metric (C(A, B)) denotes the percentage of non-dominated solutions obtained with algorithm B that are weakly dominated by non-dominated solutions obtained with algorithm A.

Algorithm	Description	Evals	Feasible	Non-dominated	$_{ m HV}$	C(A, B)
NSGA-II NSGA-II-WR	Conventional With Repair	$7,500 \\ 7,500$	5,446 7 , 500	27 59	0.7206 0.7382	0.7037 0.2034

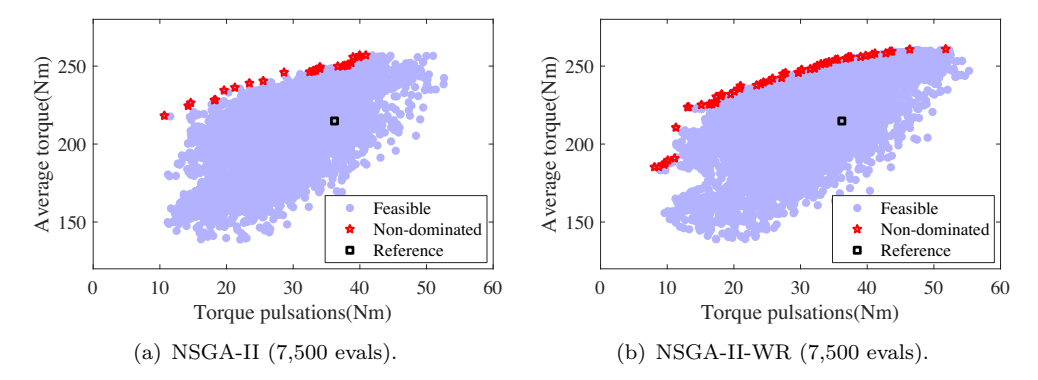


Figure 6. Objective space illustrating dominated and non-dominated (Pareto-optimal) solutions obtained with all runs combined of NSGA-II and NSGA-II-WR algorithms in (a) and (b), respectively.

5.1. Impact of Repair Operator

It is helpful first to analyze the constraints formulated in this article to understand the impact of the repair operator. A preliminary study with 10,000 randomly sampled solutions shows that only 30.3% of samples are feasible without violating any of the ten geometric constraints. Further details about the analysis of constraints are included in the supplementary document. This article investigates the impact of the repair operator by comparing two optimization methods: (1) the conventional NSGA-II and (2) NSGA-II combined with the repair operator, called NSGA-II-WR, in the rest of the article. Both methods use the simulated binary crossover (SBX) operator with a probability of 0.9 and polynomial mutation along with binary tournament selection. The distribution indices used in this study are set to $\eta_c = 15$ and $\eta_m = 20$ for crossover and mutation operators respectively. For each method, five optimization runs with different seeds are completed. However, the seeds are kept the same for the two methods for a fair comparison. Each optimization run consists of 1,500 total evaluations ($ESE^{max} = 1,500$), with a population size of 100 and 20 offsprings. Thus, five runs make up for a total of 7,500 evaluations. The two optimization methods are compared based on the combined results of the five runs, and the overall setup and details are shown in Table 2 and Figure 6. It is clear that the use of the repair operator yields more non-dominated solutions and also results in a Pareto-optimal front with larger hypervolume (HV) (Zitzler, Brockhoff, and Thiele 2007) than the conventional method. For the calculation of HV, the worst and the best points are found from the combined set of the two Pareto-optimal fronts. After that, the objective functions are normalized to obtain the normalized HV. Additionally, analysis of set coverage metric (Zitzler 1999) shows that 70% of the non-dominated solutions obtained with NSGA-II are weakly dominated by the non-dominated solutions obtained with NSGA-II-WR.

Since both methods are compared based on data from only five runs, some statistical tests can help gain more confidence in the results. For this purpose, a left-sided

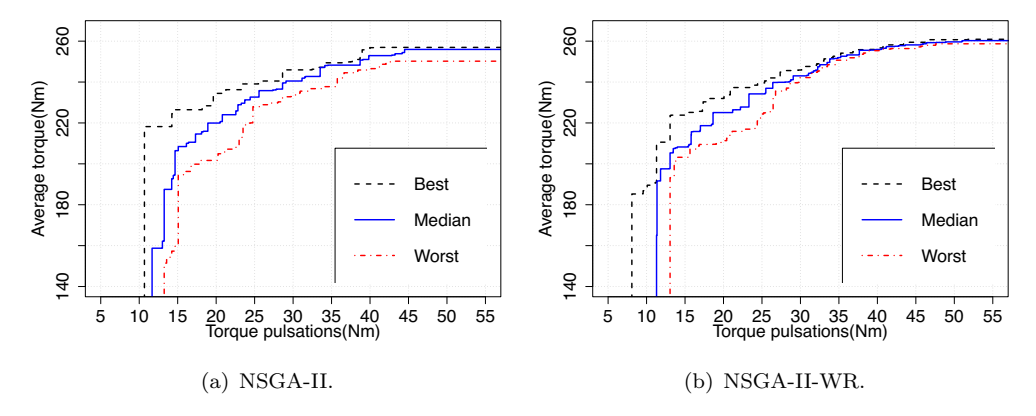


Figure 7. Objective space illustrating the best, median and worst attainment surfaces for the non-dominated (Pareto) solutions obtained from 5 runs finished with NSGA-II and NSGA-II-WR algorithms in (a) and (b), respectively.

Wilcoxon Rank sum test is performed for testing the equality of medians of the HV obtained with the two methods. The tested hypothesis is defined in (3), where \widetilde{HV}_1 and \widetilde{HV}_2 represent the median of the HV obtained from 5 runs of NSGA-II and NSGA-II-WR, respectively. At a significance level $\alpha=0.05$, the test calculates the P-value to be 0.0476, which rejects the null hypothesis H_0 and verifies that NSGA-II-WR improves the HV of the Pareto-optimal front compared to NSGA-II.

$$H_0: \widetilde{HV_1} = \widetilde{HV_2}$$

$$H_1: \widetilde{HV_1} < \widetilde{HV_2}$$

$$(3)$$

Comparing the best, median and worst attainment surfaces obtained from the non-dominated solution sets of the five runs with each method shows that NSGA-II-WR produces more consistent Pareto-optimal fronts with fewer variations (see Figure 7). Additionally, comparisons of individual runs from the two methods (included in the supplementary document) show that the Pareto-optimal fronts obtained with NSGA-II are discontinuous and mostly dominated by those obtained with NSGA-II-WR. Ultimately, the proposed repair operator is well suited for the design optimization of electric machines.

5.2. Generalizability of Repair Operator

This article investigates the generalizability of the repair operator by incorporating it into SMS-EMOA (Beume, Naujoks, and Emmerich 2007), another EMO algorithm, apart from NSGA-II. Once again, the impact of the repair operator is demonstrated by comparing the performance of (1) the conventional SMS-EMOA and (2) SMS-EMOA combined with the repair operator, called SMS-EMOA-WR, in the rest of the article. For this purpose, five optimization runs with each method are completed. Details about the optimization setup are included in the supplementary document.

The two optimization methods are compared based on the combined results of the five runs. The overall setup and results are shown in Table 3 and Figure 8. It is seen that the Pareto-optimal front obtained with SMS-EMOA has a larger HV than that with SMS-EMOA-WR (the HV calculation approach is similar to the one explained in Section 5.1). However, comparing the set coverage metric (C(A, B)) for the two

Table 3. Optimization Setup and Results for all five runs combined for SMS-EMOA and SMS-EMOA-WR. HV is calculated after normalization of objective functions. Set coverage metric (C(A, B)) denotes the percentage of non-dominated solutions obtained with algorithm B that are weakly dominated by non-dominated solutions obtained with algorithm A.

Algorithm	Description	Evals	Feasible	Non-dominated	HV	C(A, B)
SMS-EMOA	Conventional	7,500	6,573	39	0.7783 0.7615	0.8158
SMS-EMOA-WR	With Repair	7,500	7 , 500	38		0.3478

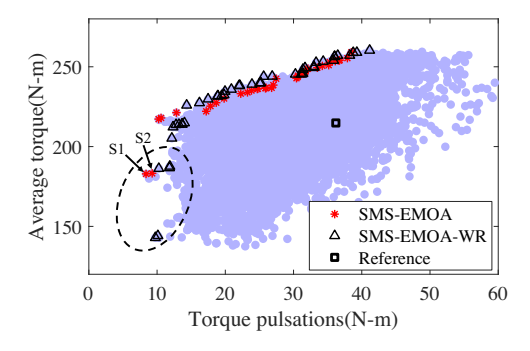


Figure 8. Objective space showing the Pareto-optimal fronts obtained by SMS-EMOA and SMS-EMOA-WR.

Pareto-optimal fronts shows that 81% of the non-dominated solutions obtained with SMS-EMOA are weakly dominated by the non-domination solutions obtained with SMS-EMOA-WR. The increased HV with SMS-EMOA can be explained by the two non-dominated solutions, S1 and S2, lying in the torque region below 200 Nm, as shown in Figure 8. However, a simple trade-off analysis between the two objectives will reveal to the user that the presence of S1 and S2, and all other non-dominated solutions lying in the region with Average torque below 200 Nm, have hardly any impact on the selection of preferred solutions. Comparing the best, median and worst attainment surfaces obtained with the two algorithms (included in the supplementary document) also verifies the superiority of the SMS-EMOA-WR. Finally, SMS-EMOA-WR outperforms the conventional SMS-EMOA and establishes the generalizability of the proposed repair operator.

5.3. Convergence Analysis With and Without Surrogates

Although surrogate-assisted optimization is known to find the Pareto-optimal front quicker than other methods, it is also sensitive to (model and optimization-related) hyperparameters. In this article, the following three hyperparameters are varied to analyze the performance of the proposed optimization method with surrogates.

- N^{ESE} : Number of ESEs in each iteration
- K: Number of surrogate optimization generations for exploitation
- N^{DOE} : Number of initial design of experiments

This parametric study's complete setup and results and some important observations are included in the supplementary document for reference. Based on this study, $N^{\text{ESE}} = 10$, K = 35, and $N^{\text{DOE}} = 60$, is identified as the best parameter setting out of the analyzed configurations. For the remainder of this article, the corresponding surrogate-assisted optimization configuration is referred to as NSGA-II-WR-SA, and its results are compared with those obtained with NSGA-II-WR. A comparison of the

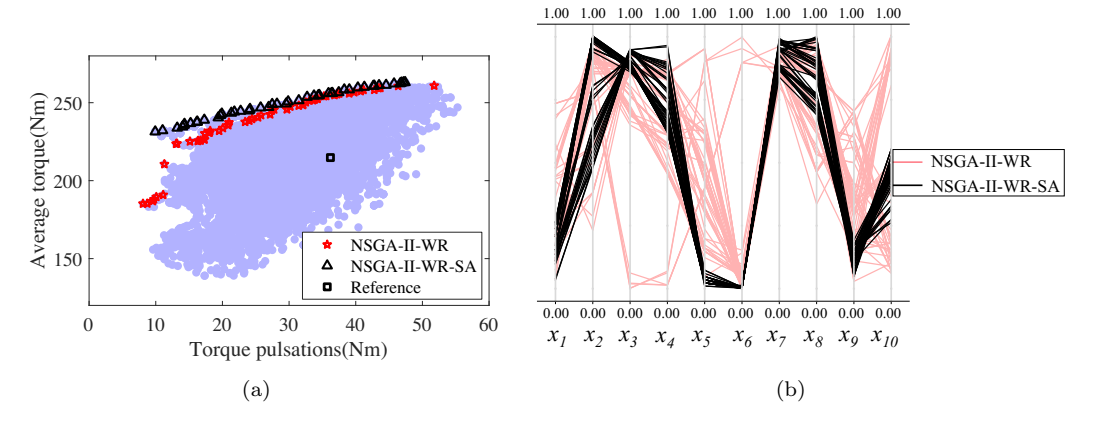


Figure 9. Comparison of objective space with Pareto-optimal fronts and normalized design space of Pareto optimal sets in (a) and (b) respectively. Pareto-optimal sets are obtained by combining all runs completed with the optimization methods, NSGA-II-WR and NSGA-II-WR-SA, respectively.

two Pareto-optimal fronts clearly shows that NSGA-II-WR-SA outperforms NSGA-II-WR, as shown in Figure 9(a). It should be noted that the compared Pareto-optimal fronts are obtained by combining all five runs for both algorithms, NSGA-II-WR and NSGA-II-WR-SA, respectively. To understand the convergence of each optimization method, the design space of the two Pareto-optimal sets is visualized by a parallel coordinates plot (PCP) (see Figure 9(b)). Each vertical axis in the PCP represents the normalized variable x_i with its lower and upper bounds as 0 and 1, respectively, and each horizontal line represents a solution.

The design space of the two Pareto-optimal sets shows that the most of the variables have converged to an optimal value with NSGA-II-WR-SA, whereas, with NSGA-II-WR, some of the variables still have significant variations with further scope for improvement. These observations validate the effectiveness of incorporating surrogates by demonstrating the improved convergence of the Pareto-optimal front. Moreover, it should be noted that while NSGA-II-WR has used 7,500 evaluations in this experiment, NSGA-II-WR-SA has converged to a better set of solutions with a solution evaluation budget of only 1,000. As explained in the previous section, surrogates are utilized to look K generations (here K=35) into the future to generate $N^{\rm ESE}$ number of infill solutions in each optimization cycle, which leads to better convergence. A comparison of individual runs included in the supplementary document further verifies the superiority of NSGA-II-WR-SA over NSGA-II-WR. Additionally, a discussion on the performance of surrogates and exploration of search space included in the supplementary document shows that convergence with surrogates depends on the complexity of the objective functions under consideration.

5.4. Analysis of Pareto-Optimal Solutions

The design space of the Pareto-optimal set obtained with NSGA-II-WR-SA is investigated to gain insights into the electric machine design (see Figure 9(b)). In general, while machine flux linkages affect the average torque, magnet pole arc and material saturation control the torque pulsations. Some critical observations are listed below.

• Most of the Pareto-optimal solutions have larger values of magnet width (x_3) , which results in more magnet flux linkage and Average torque. Larger magnet width also results in smaller q-axis width (x_6) .

- Most solutions also have larger values of slot height (x_7) and slot width (x_8) and, therefore, larger slot cross-section. A larger slot cross-section area results in more winding space, which translates to higher allowable excitation current and an increase in Average torque.
- Reduction in bridge height (x_5) directly increases the air-gap flux density, which increases Average torque.
- Magnet pole arc is directly proportional to magnet width (x_3) and angle between the magnets (x_4) , and an increase in magnet pole arc seems to decrease Torque pulsations.
- Material saturation is a nonlinear behavior observed in magnetic materials, such
 as electrical steel, introducing saturation harmonics in magnetic flux density.
 While a larger slot cross-section increases Average torque through more excitation current, it also increases magnetic material saturation, leading to more
 Torque pulsations.
- Lastly, the height and width of slot opening, x_9 and x_{10} , which are responsible for slot harmonics, have converged to the lower end of the variable ranges.

5.5. Selection of Preferred Solutions

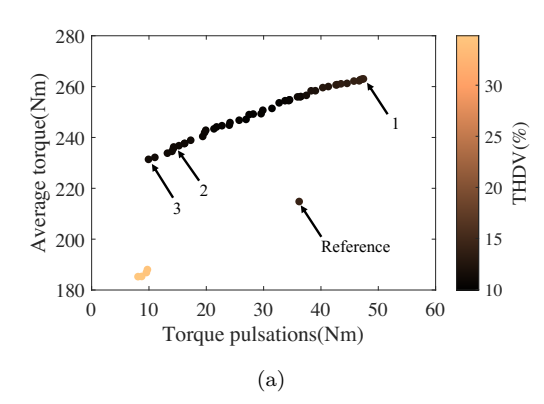
The selection of an electric machine design is primarily application-dependent. One approach could be to use a scalarized function yielding a single optimal solution (Islam, Bonthu, and Choi 2015). However, proper scalarization of objectives is a difficult task. Scalarization also does not offer the possibility of analyzing trade-offs observed for multiple objectives. Moreover, optimizing all objectives likely produces a Pareto-optimal front which is harder to interpret and gain insights into the electric machine design. This article uses two approaches to select the preferred solutions: (1) a domain-specific a posteriori MCDM method that involves machine expertise and (2) a trade-off analysis of the Pareto-optimal set to identify and choose the solutions with the highest trade-off. Both approaches use the Pareto-optimal solutions obtained from combined runs of NSGA-II-WR and NSGA-II-WR-SA algorithms.

5.5.1. Domain Specific A Posteriori MCDM Method

For a domain-specific *a posteriori* MCDM method, three performance measures, in addition to the two objective functions defined in (1), are used to select preferred solutions from the Pareto-optimal set.

- Total harmonic distortion of noload back emf (THDV)
- Peak of fundamental of back emf (F-BEMF)
- Magnet utilization factor (MUF)

Since THDV is directly proportional to noise, vibration, and harshness (NVH) during the operation of an electric machine, a solution with low THDV is desirable. Conversely, F-BEMF instead introduces a trade-off as a high F-BEMF increases Average torque, but it also leads to a reduced speed range. Lastly, a design with high MUF is desirable, where MUF is defined as the ratio of Average torque to PM volume. A primary screening based on THDV of Pareto-optimal solutions shows that the solutions lying in the bottom region of the Pareto-front must be avoided as they have more than 30% THDV, as shown in Figure 10(a). Since the remaining Pareto-optimal solutions have similar THDV (10-14%), it is easier to select solutions based on the remaining Pareto-optimal solutions, Pareto-optimal solutions, Pareto-optimal solutions have similar Pareto-optimal solutions, Pareto-optimal solutions have similar Pareto-optimal solutions, Par



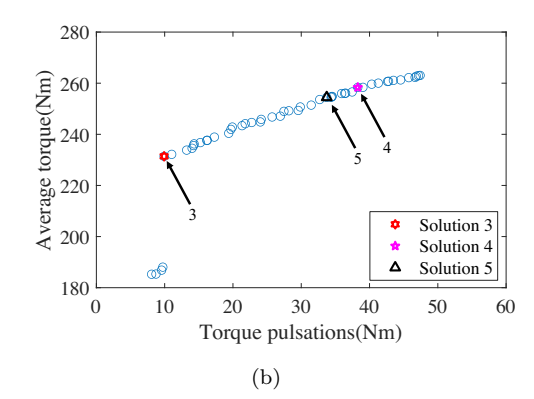


Figure 10. Objective space highlighting the selected solutions using the *a posteriori* MCDM method and trade-off analysis in (a) and (b), respectively.

Table 4. Performance comparison of the preferred solutions found using domain specific *a posteriori* MCDM method and trade-off analysis. Preferred values are highlighted in bold for the three solutions.

Solution	Average torque (Nm)	Torque pulsations (Nm)	THDV (%)	$\frac{\mathbf{MUF}}{(\mathrm{Nm}/\mathrm{mm}^3)}$	F-BEMF (V)
1	263.0374	47.4060	14.1263	0.0290	248.2401
2	235.5986	14.2488	11.2982	0.0308	236.7291
3	231.3853	9.9186	11.5016	0.0304	234.4451
Reference	214.7760	36.1846	14.4093	0.0330	209.2622

- 3, highlighted in Figure 10(a), are selected after further evaluation. The basis of the selection of the solutions is as follows.
 - Solution 1: maximum Average torque
 - Solution 2: maximum MUF
 - Solution 3: minimum Torque pulsations and F-BEMF

5.5.2. Trade-Off Calculation Using Objective Functions

A trade-off analysis of the Pareto-optimal front is an effective method for selecting preferred solutions without domain expertise. For trade-off calculation, only two objective functions defined in (1) are used, and solutions with high trade-off values are desired. The methodology for trade-off calculation is included in the supplementary document.

After performing the trade-off calculation, three solutions with the highest trade-offs, Solution 3, 4, and 5, are identified from the combined Pareto-optimal set, as shown in Figure 10(b). Interestingly, Solution 3 is picked again with the highest trade-off value (114.99). Additionally, since Solutions 4 and 5 offer a smaller trade-off value compared to Solution 3, 50.79 and 35.07, respectively, they are not considered in the rest of the discussion.

5.5.3. Performance comparison of selected solutions

Performance details of the selected solutions and the reference design are given in Table 4. Further insights into the performance of these solutions can be gained by analyzing the design space, as shown in Figure 11(a). Some essential observations highlighting the trade-off among selected solutions are as follows.

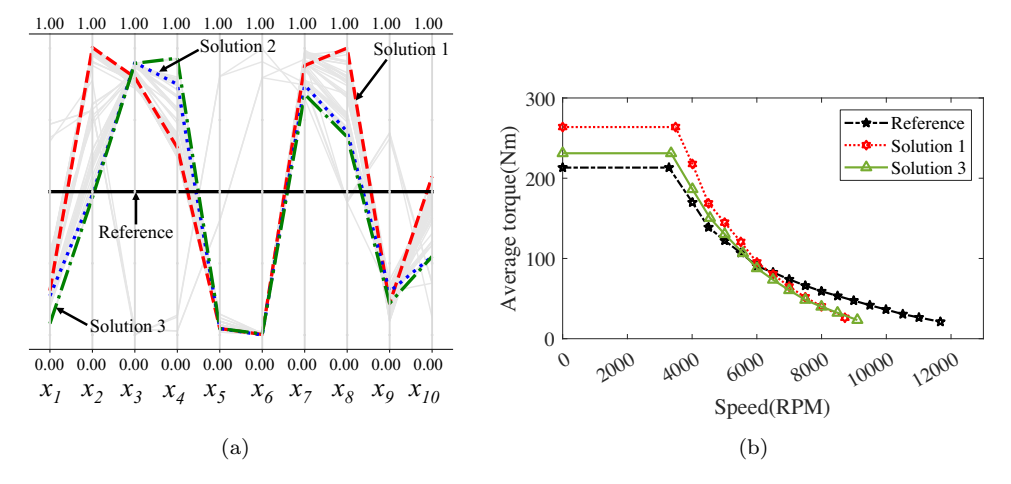


Figure 11. Selected Pareto-optimal solutions are highlighted in normalized design space in (a). Torque-speed curve of reference design and solutions 1 and 3 is shown in (b).

- Although Solution 1 provides maximum Average torque; it also has the maximum amplitude of Torque pulsations and F-BEMF. Both these characteristics can be explained by larger magnet thickness (x_2) , slot height (x_7) , slot width (x_8) , and slot opening height and width (x_9) and (x_{10}) .
- Solutions 2 and 3 perform quite similarly in all aspects, with slight variations observed in Average torque and Torque pulsations. This variation is caused by the different angles between magnets (x_4) observed for the two solutions.
- All selected solutions have a larger F-BEMF value compared to the reference design. In other words, they have a lower speed range. The relation between F-BEMF and the maximum achievable speed is illustrated in Figure 11(b). With further increase in speeds, one would observe that torque produced by Solution 1 drops to zero more quickly compared to Solution 3. Since Solutions 2 and 3 have similar F-BEMF, their torque/speed profiles are also expected to be similar.
- A comparison of the magnetic flux density plots of Solutions 1, 2, and 3 at corresponding rated operating conditions reveals that Solution 1 suffers from higher saturation in stator teeth, back iron, and rotor steel close to magnet edges (see Figure 12).

Based on this in-depth discussion, one should select Solution 1 for an application with a high Average torque requirement. If the focus is more on a smooth operation with a high-speed range, Solution 2 or 3 should be chosen. It is also worth mentioning that while the trade-off analysis can pick Solution 3, it does not pick Solution 2 with the highest MUF, but can be selected by utilizing domain expertise. Ultimately, selecting a single solution out of a Pareto-optimal set is a difficult task that can often be alleviated using the machine designer's experience.

6. Conclusion

This article has investigated a bi-objective electric machine design optimization problem with geometric constraints. While the geometric constraints are evaluated using analytical expressions, the objective functions require costly finite element analysis, leading to a mixed computationally expensive optimization problem. The proposed

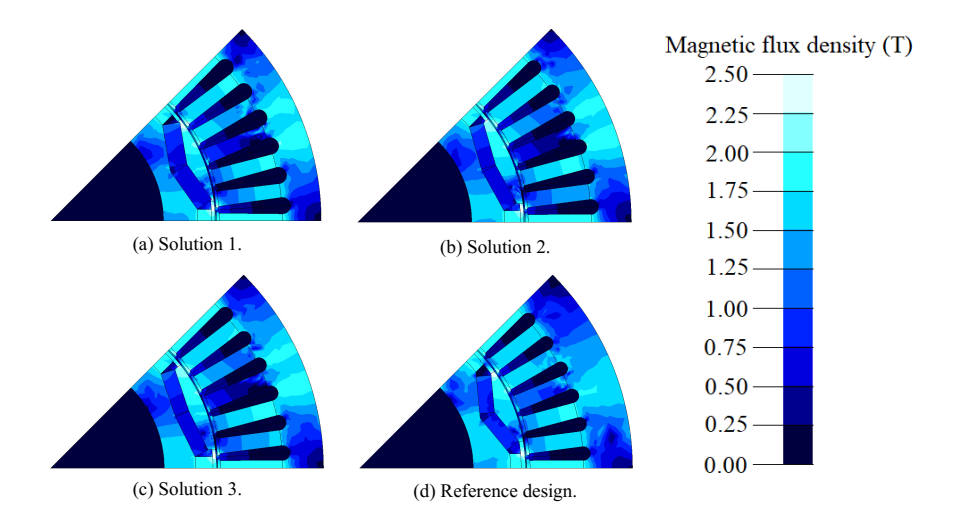


Figure 12. Magnetic flux density plots of Solutions 1, 2, 3 and reference design at rated operation.

method has used a repair operator to handle inexpensive constraints and surrogate models to predict expensive objectives. Both concepts have been integrated into a well-known evolutionary multi-objective optimization (EMO) algorithm: NSGA-II. Infeasible solutions have been replaced with repaired feasible solutions, thereby ensuring feasibility during optimization. This article has also verified the generalizability of the proposed repair operator by incorporating it into another EMO algorithm: SMS-EMOA. Moreover, the surrogate incorporation has been analyzed in-depth and shown to be critical for improving efficiency. First, surrogate-related parameters have been investigated by performing a sequential parametric study, examining the number of infill solutions in each generation (N^{ESE}), the number of generations for exploiting the surrogate model (K), and the number of the initial design of experiments (N^{DOE}). The parametric study has provided a suitable configuration for solving this electric machine design problem. Results have validated the superiority of incorporating surrogates by improving the algorithm's convergence even with fewer expensive evaluations.

The ultimate goal of an optimization task is to reach an optimal solution that can be implemented successfully. Unlike many other applied multi-objective optimization studies, this article has presented a domain-specific a posteriori MCDM approach focusing on the machine cost, noise, vibration, and harshness (NVH) issues, and speed range of the electric machine to choose a single preferred solution. The presented a posteriori selection approach has identified the trade-off offered by different Pareto-optimal solutions and facilitated the selection of a handful of optimized electric machine designs. Additionally, a trade-off analysis based on objective vectors has been performed to select preferred solutions, helping the user to systematically identify a few critical designs from a large search space.

Future research should now be conducted on an approach to perform parameter tuning automatically. Integrating a repair operator and surrogate models into an EMO algorithm has shown promising results for optimizing electric machine designs. However, more application problems having a computationally mixed expensive nature need to be investigated. Nevertheless, this study has shown the advantage of using a flexible EMO algorithm with efficient handling of constraints and using surrogates for expensive evaluation procedures to discover a diverse set of high-performing designs. The study has also revealed a set of key design principles common to multiple high-

performing designs for enhancing knowledge about the problem and demonstrated the use of MCDM approaches to choose one or a few preferred solutions for implementation. The complete optimization-cum-decision-making on a complex electric motor design problem demonstrated in this study should pave the way for applying similar procedures in other engineering design optimization tasks.

7. Data Availability Statement

The data that support the findings of this study are available from the corresponding author upon reasonable request.

8. Disclosure Statement

No potential competing interest was reported by the authors.

References

- Aggarwal, Anmol, Ibrahim Mahmood Allafi, Elias G. Strangas, and John S. Agapiou. 2021. "Off-Line Detection of Static Eccentricity of PMSM Robust to Machine Operating Temperature and Rotor Position Misalignment Using Incremental Inductance Approach." *IEEE Transactions on Transportation Electrification* 7 (1): 161–169.
- Aggarwal, Anmol, Elias G. Strangas, and John Agapiou. 2019a. "Analysis of Unbalanced Magnetic Pull in PMSM Due to Static Eccentricity." 2019 IEEE Energy Conversion Congress and Exposition (ECCE) 4507–4514.
- Aggarwal, Anmol, Elias G. Strangas, and John Agapiou. 2019b. "Robust Voltage based Technique for Automatic Off-Line Detection of Static Eccentricity of PMSM." 2019 IEEE International Electric Machines & Drives Conference (IEMDC) 351–358.
- Aggarwal, Anmol, Elias G. Strangas, and Athanasios Karlis. 2020. "Review of Segmented Stator and Rotor Designs for AC Electric Machines." 2020 International Conference on Electrical Machines (ICEM) 2342–2348.
- Beume, Nicola, Boris Naujoks, and Michael Emmerich. 2007. "SMS-EMOA: Multiobjective selection based on dominated hypervolume." *European Journal of Operational Research* 181 (3): 1653-1669. https://www.sciencedirect.com/science/article/pii/S0377221706005443.
- Bianchi, N., and S. Bolognani. 1998. "Design optimisation of electric motors by genetic algorithms." *IEE Proceedings Electric Power Applications* 145: 475-483(8). https://digital-library.theiet.org/content/journals/10.1049/ip-epa_19982166.
- Blank, J., and K. Deb. 2021. "Constrained bi-objective surrogate-assisted optimization of problems with heterogeneous evaluation times: Expensive objectives and inexpensive constraints." In *Evolutionary multi-criterion optimization*, edited by Hisao Ishibuchi, Qingfu Zhang, Ran Cheng, Ke Li, Hui Li, Handing Wang, and Aimin Zhou, 257–269. Springer International Publishing.
- Blank, Julian, and Kalyanmoy Deb. 2022. "pysamoo: Surrogate-Assisted Multi-Objective Optimization in Python." .
- Deb, K., R. Hussein, P. C. Roy, and G. Toscano-Pulido. 2019. "A taxonomy for metamodeling frameworks for evolutionary multiobjective optimization." *IEEE Transactions on Evolutionary Computation* 23 (1): 104–116.
- Deb, K., A. Pratap, S. Agarwal, and T. Meyarivan. 2002. "A fast and elitist multiobjective genetic algorithm: NSGA-II." *IEEE Transactions on Evolutionary Computation* 6 (2): 182–197.

- Deb, Kalyanmoy. 2001. Multi-Objective Optimization Using Evolutionary Algorithms. USA: John Wiley & Sons, Inc.
- Degano, M., M. Di Nardo, M. Galea, C. Gerada, and D. Gerada. 2016. "Global design optimization strategy of a synchronous reluctance machine for light electric vehicles." In 8th IET International Conference on Power Electronics, Machines and Drives (PEMD 2016), 1–5.
- Duan, Y., R. G. Harley, and T. G. Habetler. 2009. "Comparison of particle swarm optimization and genetic algorithm in the design of permanent magnet motors." 2009 IEEE 6th International Power Electronics and Motion Control Conference, IPEMC '09 3: 822–825.
- Duan, Yao, and Dan M. Ionel. 2013. "A review of recent developments in electrical machine design optimization methods with a permanent-magnet synchronous motor benchmark study." *IEEE Transactions on Industry Applications* 49 (3): 1268–1275.
- Flux, Altair. 2019. Altair Flux (Version 2019.1). Altair Engineering Inc. https://www.altair.com/flux/.
- FluxMotor, Altair. 2019. Altair FluxMotor (Version 2019.1.1). Altair Engineering Inc. https://www.altair.com/fluxmotor/.
- Hardy, Rolland L. 1971. "Multiquadric equations of topography and other irregular surfaces." *Journal of Geophysical Research* (1896-1977) 76 (8): 1905–1915. Accessed 2020-10-06. https://doi.org/10.1029/JB076i008p01905.
- Hayslett, Steven, Thang Pham, and Elias Strangas. 2022. "Analytical Minimization of Interior Permanent Magnet Machine Torque Pulsations by Design of Sculpted Rotor." *Energies* 15 (11). https://www.mdpi.com/1996-1073/15/11/4124.
- Hayslett, Steven, and Elias Strangas. 2021. "Analytical Design of Sculpted Rotor Interior Permanent Magnet Machines." *Energies* 14 (16). https://www.mdpi.com/1996-1073/14/16/5109.
- Hooke, Robert, and T. A. Jeeves. 1961. "" Direct Search" Solution of Numerical and Statistical Problems." *J. ACM* 8: 212–229.
- Huang, Shaopo, Anmol Aggarwal, Elias G. Strangas, Kui Li, Feng Niu, and Xiaoyan Huang. 2021. "Robust Stator Winding Fault Detection in PMSMs With Respect to Current Controller Bandwidth." *IEEE Transactions on Power Electronics* 36 (5): 5032–5042.
- Huang, Shaopo, Elias G. Strangas, Anmol Aggarwal, Kui Li, and Feng Niu. 2019. "Robust Inter-turn Short-circuit Detection in PMSMs with Respect to Current Controller Bandwidth." 2019 IEEE Energy Conversion Congress and Exposition (ECCE) 3897–3904.
- Ionel, Dan M., and Mircea Popescu. 2009. "Finite element surrogate model for electric machines with revolving field application to IPM motors." In 2009 IEEE Energy Conversion Congress and Exposition, 178–186.
- Islam, Md. Zakirul, Sai Sudheer Reddy Bonthu, and Seungdeog Choi. 2015. "Obtaining optimized designs of multi-phase PMa-SynRM using lumped parameter model based optimizer." In 2015 IEEE International Electric Machines Drives Conference (IEMDC), 1722–1728.
- Jolly, L., M.A. Jabbar, and Liu Qinghua. 2005. "Design optimization of permanent magnet motors using response surface methodology and genetic algorithms." *IEEE Transactions on Magnetics* 41 (10): 3928–3930.
- Khoshoo, Bhuvan, Julian Blank, Thang Pham, Kalyanmoy Deb, and Shanelle Foster. 2021. "Optimized Electric Machine Design Solutions with Efficient Handling of Constraints." In 2021 IEEE Symposium Series on Computational Intelligence (SSCI), 1–8.
- Khoshoo, Bhuvan, Orwell Madovi, Anmol Aggarwal, and Shanelle N. Foster. 2022. "Impact of Rotor Segmentation on Electromagnetic Performance of PM Machine." In 2022 International Conference on Electrical, Computer and Energy Technologies (ICECET), 1–7.
- Krige, D. G. 1951. "A statistical approach to some basic mine valuation problems on the Witwatersrand, by D.G. Krige, published in the Journal, December 1951: introduction by the author.".
- Mirzaeian, B., M. Moallem, V. Tahani, and C. Lucas. 2002. "Multiobjective optimization method based on a genetic algorithm for switched reluctance motor design." *IEEE Transactions on Magnetics* 38 (3): 1524–1527.

- Nelder, J. A., and R. Mead. 1965. "A Simplex Method for Function Minimization." Computer Journal 7: 308–313.
- Pellegrino, G., and F. Cupertino. 2010a. "FEA-based multi-objective optimization of IPM motor design including rotor losses." In 2010 IEEE Energy Conversion Congress and Exposition, 3659–3666.
- Pellegrino, G., and F. Cupertino. 2010b. "IPM motor rotor design by means of FEA-based multi-objective optimization." In 2010 IEEE International Symposium on Industrial Electronics, 1340–1346.
- Pellegrino, Gianmario, Francesco Cupertino, and Chris Gerada. 2015. "Automatic Design of Synchronous Reluctance Motors Focusing on Barrier Shape Optimization." *IEEE Transactions on Industry Applications* 51 (2): 1465–1474.
- Ramarathnam, R., B. G. Desai, and V. Subba Rao. 1973. "A Comparative Study of Minimization Techniques for Optimization of Induction Motor Design." *IEEE Transactions on Power Apparatus and Systems* PAS-92 (5): 1448–1454.
- Sasena, Michael J. 2002. "Flexibility and efficiency enhancements for constrained global design optimization with kriging approximations." PhD diss. Copyright Database copyright ProQuest LLC; ProQuest does not claim copyright in the individual underlying works; Last updated 2022-01-05, http://ezproxy.msu.edu/login?url=https://www.proquest.com/dissertations-theses/flexibility-efficiency-enhancements-constrained/docview/276318341/se-2.
- Singh, Bhim, B. P. Singh, S. S. Murthy, and C. S. Jha. 1983. "Experience in Design Optimization of Induction Motor Using 'SUMT' Algorithm." *IEEE Transactions on Power Apparatus and Systems* PAS-102 (10): 3379–3384.
- Sizov, Gennadi Y., Dan M. Ionel, and Nabeel A. O. Demerdash. 2012. "Modeling and Parametric Design of Permanent-Magnet AC Machines Using Computationally Efficient Finite-Element Analysis." *IEEE Transactions on Industrial Electronics* 59 (6): 2403–2413.
- Song, Juncai, Jiwen Zhao, Fei Dong, Jing Zhao, Zhe Qian, and Qian Zhang. 2018. "A Novel Regression Modeling Method for PMSLM Structural Design Optimization Using a Distance-Weighted KNN Algorithm." *IEEE Transactions on Industry Applications* 54 (5): 4198–4206.
- Stipetic, Stjepan, Werner Miebach, and Damir Zarko. 2015. "Optimization in design of electric machines: Methodology and workflow." In 2015 Intl Aegean Conference on Electrical Machines Power Electronics (ACEMP), 2015 Intl Conference on Optimization of Electrical Electronic Equipment (OPTIM) 2015 Intl Symposium on Advanced Electromechanical Motion Systems (ELECTROMOTION), 441–448.
- Sudhoff, Scott D., James Cale, Brandon Cassimere, and Mike Swinney. 2005. "Genetic algorithm based design of a permanent magnet synchronous machine." 2005 IEEE International Conference on Electric Machines and Drives 1011–1019.
- Taran, Narges, Dan M. Ionel, and David G. Dorrell. 2018. "Two-Level Surrogate-Assisted Differential Evolution Multi-Objective Optimization of Electric Machines Using 3-D FEA." *IEEE Transactions on Magnetics* 54 (11): 1–5.
- Žarko, Damir, Drago Ban, and Thomas A. Lipo. 2005. "Design optimization of Interior Permanent Magnet (IPM) motors with maximized torque output in the entire speed range." 2005 European Conference on Power Electronics and Applications 2005.
- Zhang, Peng, Gennadi Y. Sizov, Dan M. Ionel, and Nabeel A.O. Demerdash. 2013. "Design optimization of spoke-type ferrite magnet machines by combined design of experiments and differential evolution algorithms." In 2013 International Electric Machines Drives Conference, 892–898.
- Zitzler, Eckart. 1999. "Evolutionary algorithms for multiobjective optimization: methods and applications.".
- Zitzler, Eckart, Dimo Brockhoff, and Lothar Thiele. 2007. "The Hypervolume Indicator Revisited: On the Design of Pareto-compliant Indicators Via Weighted Integration." In *Evolutionary Multi-Criterion Optimization*, edited by Shigeru Obayashi, Kalyanmoy Deb, Carlo Poloni, Tomoyuki Hiroyasu, and Tadahiko Murata, Berlin, Heidelberg, 862–876. Springer Berlin Heidelberg.